UPDATED THEORY OF THE X-RAY DIFFRACTION RESIDUAL STRESS MEASUREMENT COMPARING COS-ALPHA AND SIN²PSI TECHNIQUES – BIAXIAL VERSUS TRIAXIAL

Mohammed Belassel[1], James Pineault[1], Michael Brauss[2]

[1] PROTO MANUFACTURING LIMITED, Canada
[2] PROTO MANUFACTURING INC, USA

Abstract
When applying the $Sin^2\psi$ technique to x-ray diffraction (XRD) based residual stress measurements, both the normal and shear stress components can be easily and accurately evaluated in the direction(s) of interest. The $Sin^2\psi$ technique was developed and refined over several decades along with many other advances so as to achieve high accuracy residual stress measurement results in a wide variety of circumstances and material conditions. With the introduction of the $Cos\alpha$ technique, only the biaxial stress field was considered in the calculation of the stress tensor components and as such, is susceptible to significant errors often resulting in unreliable residual stress measurements. In the present study, the $Sin^2\psi$ and $Cos\alpha$ techniques were compared and evaluated. It is shown that the biaxial based $Cos\alpha$ technique leads to erroneous stress data when in-plane shear stress is present, and results are found to be equivalent to the two-tilt $Sin^2\psi$ technique. In other words, the $Cos\alpha$ technique used in only one orientation could not reproduce the correct results as obtained via the $Sin^2\psi$ technique with multiple tilts. Thus, the only viable solution is to assume a triaxial stress tensor and to collect data with tilts distributed evenly over the half-space when using the $Cos\alpha$ technique.

Keywords: Residual Stress, Shear stress, CosAlpha, Single Exposure, Sin^2Psi, Standard

Introduction

The development of residual stress measurements using x-ray diffraction techniques went through many steps over time. Initially, the residual stress field was assumed to be biaxial because of the stress boundary conditions and the shallow penetration of x-rays. Therefore, all stress components in the third direction were assumed to be zero, i.e., σ_{i3}=0. [1]. At the time, stress measurements were only executed using positive inclination angles (ψ^+) while a linear regression was sufficient to determine the normal stress in the direction of interest (ϕ=0°). As a result, the design of instruments was tailored to accommodate the biaxial stress tensor assumption. However, it was known that misalignment of the goniometer resulting in a beam shift would cause PSI-Splitting when measuring both the (ψ^+) and (ψ-) branches [2]. The common practice was to flip the component (ϕ=180°) exclusively to verify the misalignment of the goniometer.

The first time PSI-Splitting was recorded on a component, it was reported in a task force residual stress meeting [2]. After double verification of the alignment, it was established that the shear stress was indeed real, and that it originated from the processing of the component itself, not the misalignment of the goniometer. Since then, the scientific community has established a new reliable procedure to measure residual stresses in materials using the $Sin^2\psi$ technique assuming a triaxial stress tensor. Many advances have been introduced over the last several decades which have resulted in the development of thorough and well documented residual stress standards and best practice guidelines that enable high accuracy and reliable residual stress measurements using XRD [3,4].

With the emergence and development of the $Cos\alpha$ technique using a 2D detector, the biaxial stress tensor was the prime assumption included in all marketed instruments [5]. However, this technique was found to exhibit many limitations and weaknesses in addition to the ones already

known for all XRD techniques in general. Moreover, it has been shown that the Cosα technique suffers from the exact same limitations as the two-tilt Sin²ψ technique (SET- Sin²ψ) [6,7]. The Cosα technique cannot reliably measure stresses in materials when anisotropy and in-plane shear stresses (τ_{13} or τ_{23}) exist because their presence produces a significant effect that can easily mislead a measurement practitioner [7].
To demonstrate the need to use a triaxial stress tensor in the stress model, a simulation comparing the following techniques was developed: 1) the Sin²ψ technique with multiple tilt angles (MET- Sin²ψ), 2) the Sin²ψ technique with two tilt angles (SET- Sin²ψ), and 3) the Cosα technique with a single tilt (SET-Cosα). This work emphasizes the limitations of the SET- Sin²ψ and the Cosα techniques along with the effect of different measurement conditions on the stress results obtained.

Shear stress induced processes
The in-plane shear stress is a result of non-uniform processes applied to materials exhibiting heterogeneous microstructure including ferrous alloys. These processes are many, among them, machining, grinding, roll-peening, friction and directional peening. Other shear stresses are fictitious and can be generated from a curved geometry or tilted surface. All of these shear stresses will affect the calculation of the normal stress component [2].

Cos-Alpha techniques
The Cosα residual stress measurement technique is XRD based and uses the distance between crystallographic planes (i.e., the d-spacing) as a strain gauge. It can only be applied to crystalline, polycrystalline, and semi-crystalline materials [1,2]. When the material is in tension, the d-spacing increases and when the material is in compression, the d-spacing decreases. The d-spacing is calculated from the measured Bragg angle 2θ for a known x-ray wavelength λ using Bragg's law:

$$n\lambda = 2d\sin\theta \qquad (1)$$

Subsequently, the strain ε is calculated from unstressed (d_0) and stressed ($d_{\psi\varphi}$) values for each orientation defined by the angles ϕ and ψ. Hence the strain is calculated using the following relationship:

$$\varepsilon_{\varphi\psi} = \frac{d_{\varphi\psi} - d_0}{d_0} \qquad (2)$$

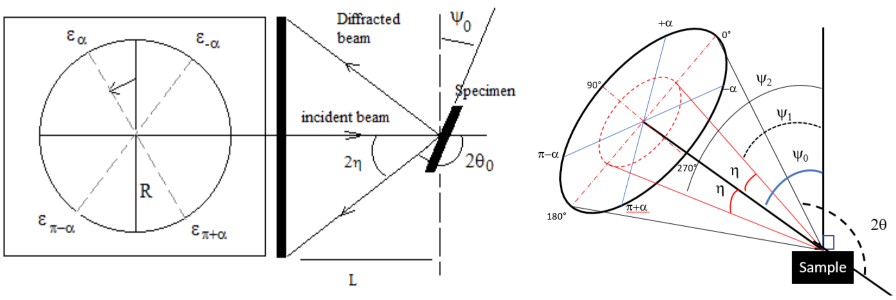

Figure 1: SET-Cosα technique geometry using full Debye ring.

Cosα technique uses the whole Debye ring collected with a 2D detector, and determines the peak position for each angle α around the ring [5]. ψ_0 is the inclination of the sample relative to the incident beam, ϕ_0 is the direction of the measurement, and 2η is the angle subtended by the incident and diffracted beams. The tilting angles are therefore defined as: $\psi_1 = \psi_0 + \eta$, and $\psi_2 = \psi_0 - \eta$, where $\eta = (\pi - 2\theta)/2$ (see Figure 1). Strain quantities can be defined as shown in the Eq. 3 and 4:

$$a_1 = \frac{1}{2}[(\varepsilon_\alpha - \varepsilon_{\pi+\alpha}) + (\varepsilon_{-\alpha} - \varepsilon_{\pi-\alpha})] \qquad (3)$$

$$a_2 = \frac{1}{2}[(\varepsilon_\alpha - \varepsilon_{\pi+\alpha}) - (\varepsilon_{-\alpha} - \varepsilon_{\pi-\alpha})] \quad (4)$$

where ε_α, $\varepsilon_{\pi+\alpha}$, $\varepsilon_{-\alpha}$, and $\varepsilon_{\pi-\alpha}$ are the measured strains from the four sectors of the Debye ring. For $\phi_0 = 0$, the direction of the strain can be reduced to the following expression:

$$n_i = \begin{pmatrix} cos\eta \; sin\psi_0 + sin\eta \; cos\psi_0 \; cos\alpha \\ sin\eta \; sin\alpha \\ cos\eta \; cos\psi_0 - sin\eta \; sin\psi_0 cos\alpha \end{pmatrix} \quad (5)$$

Considering Triaxial stress tensor

Considering a triaxial stress field, new expressions are derived for a_1 and a_2:

$$a_1 = -\frac{(1+\upsilon)}{E}(\sigma_{11} sin2\psi_0 - 2\tau_{13} cos2\psi_0) sin2\eta . Cos\alpha \quad (6)$$

$$a_2 = \frac{2(1+\upsilon)}{E}(\tau_{12} sin\psi_0 + 2\tau_{23} cos\psi_0) sin2\eta . Sin\alpha \quad (7)$$

And the stress terms are calculated for the slopes of a_1=f(Cosα) and a_2=f(Sinα) as follows:

$$(\sigma_{11} sin2\psi_0 - 2\tau_{13} cos2\psi_0) = -\frac{E}{(1+\upsilon) sin2\eta}\frac{\partial a_1}{\partial Cos\alpha} \quad (8)$$

$$(\tau_{12} sin\psi_0 + 2\tau_{23} cos\psi_0) = \frac{E}{2(1+\upsilon) sin2\eta}\frac{\partial a_2}{\partial Sin\alpha} \quad (9)$$

Since most polycrystalline materials are considered anisotropic, Young's modulus, E, and Poisson's ratio ν, are replaced by ½S_2 and S_1 using the following expressions [1]:

$$\frac{1+\upsilon}{E} = ½ S_2 \text{ and } \frac{\upsilon}{E} = S_1 \quad (10)$$

To solve Eq. 8 and 9 for all 4 components (σ_{11}, τ_{13}) and (τ_{12}, τ_{23}), a set of 4 equations are necessary. This will require at least two measurements, i.e., 2-Debye rings [10]. For better statistical sampling, more tilts are recommended.

Considering the Biaxial stress tensor

For the biaxial stress tensor, the second terms in Eq. 8 and 9 are dropped therefore the new equations are:

$$(\sigma_{11}) = -\frac{E}{(1+\upsilon). sin2\psi_0 . sin2\eta}\frac{\partial a_1}{\partial Cos\alpha} \quad (11)$$

$$(\tau_{12}) = \frac{E}{2(1+\upsilon). sin\psi_0 . sin2\eta}\frac{\partial a_2}{\partial Sin\alpha} \quad (12)$$

The components σ_{11} and τ_{12}, in this case, can be calculated from a single Debye ring data. Cosα instruments that use by default only one Debye ring assume a biaxial stress tensor and therefore, cannot calculate the shear components (τ_{13}, τ_{23}).

Sin²ψ Technique – Multiple Exposure Technique (MET-Sin²ψ)

The constitutive equations for the Sin$^2\psi$ technique are as follows [1]:

$$\varepsilon_{\varphi\psi} = \frac{1+\upsilon}{E}(\sigma_{11} cos^2\varphi + \sigma_{22} sin^2\varphi + \tau_{12} sin2\varphi) Sin^2\psi$$
$$-\frac{\upsilon}{E}(\sigma_{11} + \sigma_{22}) + \frac{1+\upsilon}{E}(\tau_{13} cos\varphi + \tau_{23} sin\varphi) Sin2\psi \quad (13)$$

The normal stress in the direction of interest, φ, can be defined as:

$$\sigma^\varphi = \sigma_{11} cos^2\varphi + \sigma_{22} sin^2\varphi + \tau_{12} sin2\varphi \quad (14)$$

$$\tau^\varphi = \tau_{13} cos\varphi + \tau_{23} sin\varphi \quad (15)$$

All stress components can be calculated from a triaxial measurement with multiple (φ,ψ) directions or (σ_{11}, τ_{13}) from a single measurement with multiple tilts. The normal and shear stresses are independent and can be calculated using either a linear or elliptical fit. It is recommended that when using this technique, both positive and negative ψ-angles ranging from +45º to -45º are covered, and that at least 9 tilts distributed approximately equally be sampled [4].

Two-tilt method Sin²ψ (SET-Sin²ψ)
The SET-Sin^{2}ψ technique in this case uses a single goniometer tilt with two detectors, which is equivalent to using 2 goniometer tilts with one detector (i.e. both scenarios sample two different ψ angles). In general, a single tilt is used with two detectors where the angles are defined as: ψ_1 and ψ_2 defined in SET-Cosα paragraph [1]. These angles correspond to α =0° and α =180° on the Debye ring (see Figure 1). For the SET-Sin^{2}ψ, Eq. 13 can be reduced to the following equation with $\sigma_{22}=\sigma_{33}=\tau_{13}=0$ and $\phi=0º$:

$$\sigma^{\varphi} = \sigma_{11} = \frac{\partial \varepsilon_{\psi}}{\partial Sin^2\psi}\frac{E}{1+\upsilon} \quad (16)$$

Given these assumptions, when using the SET-Sin^{2}ψ, only one normal stress component (σ^{φ}) can be determined.

Residual stress simulation
In order to demonstrate the limitations of both the SET-Cosα technique and the SET-Sin^{2}ψ technique, a theoretical approach was opted for using simulation since it is advantageous for studying a variety of parameters. The simulation method was described in [7] and it consists of calculating the stress values from a known initial input stress tensor σ_{ij} then the strains $\varepsilon_{\varphi\psi\alpha}$ in every direction for all 3 techniques: SET-Cosα, SET-Sin^{2}ψ and MET-Sin^{2}ψ. This simulation illustrates the effect of the inclination angle ψ_0 on the normal stress, the stress error due to the presence of shear stress, stress evolution under load, and the residual stress value offset due to the presence of shear stress.

Parameters influencing the SET-Cosα technique

Tilting angle:
As illustrated in Eq. 8 and 9, the stress value is directly dependent on the values of the tilt angle ψ_0 and the magnitude of shear stress present. The normal stress (σ_{11}) is directly affected by the magnitude of the τ_{13}, and τ_{23} shear stress components as illustrated in Figure 2. These residual stresses were simulated for both the positive and the negative ψ-tilts and for two different magnitudes of shear stress as shown in the stress tensors below:

$$\sigma_{ij}(\text{MPa})=\begin{pmatrix}500 & 100 & 100\\ 100 & 500 & 100\\ 100 & 100 & 0\end{pmatrix} \text{ and } \sigma_{ij}(\text{MPa})=\begin{pmatrix}500 & 100 & 50\\ 100 & 500 & 50\\ 50 & 50 & 0\end{pmatrix}$$

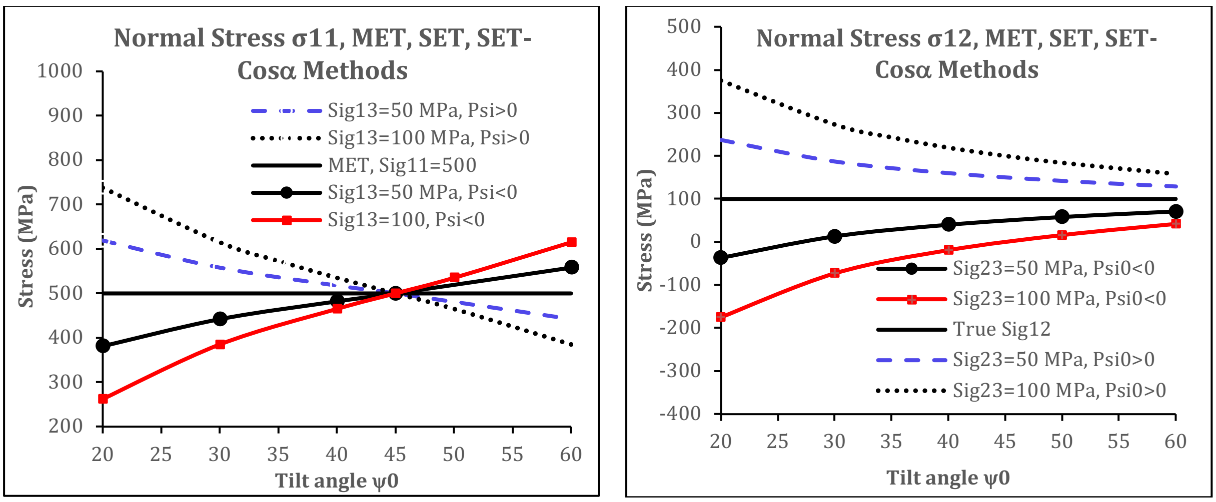

Figure 2: Simulated stress tensor terms σ_{11} and τ_{12} versus ψ_0, for both ψ_0<0 and ψ_0>0 values using: SET-Cosα,SET-Sin^{2}ψ, and MET-Sin^{2}ψ, for 2 different stress tensor inputs.

These simulation results indicate that the presence of the shear stresses τ_{13} and/or τ_{23} are expected to offset both the σ_{11} and τ_{12} stress components that the SET-Cosα technique produces. This effect has been confirmed experimentally [6,9]. The offset for σ_{11} varies with both the direction and the magnitude of ψ-tilt angle. It is only at ψ_0=45° where the shear stress effect is eliminated. The magnitude of residual stresses can be either overestimated or underestimated, depending on the orientation of the part and the sign of the shear stress component. Both components σ_{11} and τ_{12} converge to their true values of 500 MPa and 100 MPa when the ψ-tilt angles are ±45° and ±90° respectively. The influence of τ_{23} on τ_{12} is most significant when the stress levels are on the same order of magnitude. The effect of the tensor terms τ_{13} and τ_{23} on σ_{11} and τ_{12} respectively are independent, however, the presence of τ_{23} will affect σ_{22} when measured in the ϕ_0=90°direction.

Shear stress levels:

The absolute errors on the normal stress σ_{11} and the shear stress τ_{12} are proportional to the magnitude of the shear stress only (not the magnitude of the normal stress), and the relative error is inversely proportional to the normal residual stress magnitude. Therefore, the relative stress error is inversely proportional to the magnitude of the shear stress (see Figure 3).

High shear stress magnitudes can easily be generated in ground and machined materials or components while still having relatively low magnitude normal stress values. The stress errors in such cases can be significant and cannot be discounted. Moreover, the shear stress τ_{12} is highly altered by the presence of the shear stress τ_{23} and as such, can have huge implications when considering principal stress calculations.

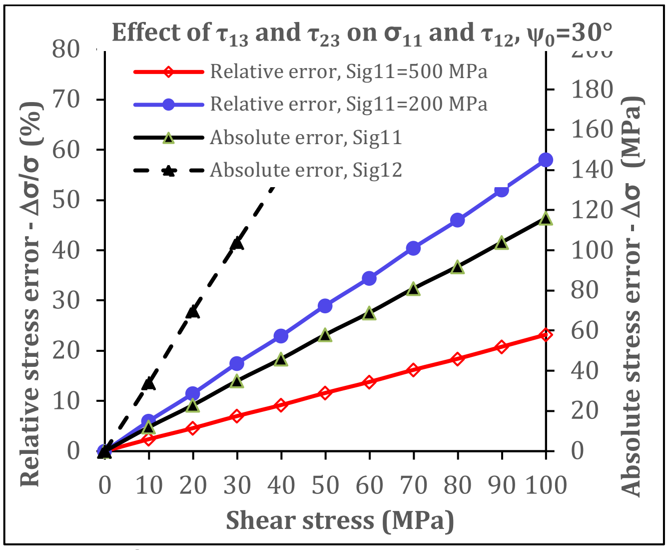

Figure 3: Simulated normal stress errors caused by the presence of the τ_{13} and τ_{23} shear stress components at different levels [8].

Presence of Anisotropy

All residual stress measurement techniques (including XRD) are sensitive to the microstructure present in the material including grain size and preferred orientation. As such, accurate residual stress measurements must be able to account for, and consider, the effect of the material microstructure. Sin²ψ, state-of-the-art goniometers and software are generally equipped with tools to mitigate and/or eliminate these effects. However, the SET-Cosα technique does not enjoy these advantages and it is often either very difficult or impossible to equate SET-Cosα to MET-Sin²ψ results when grain size and preferred orientation effects are present. Depending on the severity of these factors, SET-Cosα stress results can be completely erroneous. These effects are illustrated in the example shown in Figure 4. When comparing these two techniques side by side, the MET-Sin²ψ technique has been shown to produce reasonably accurate results, whereas the SET-Cosα technique fails completely [7,11].

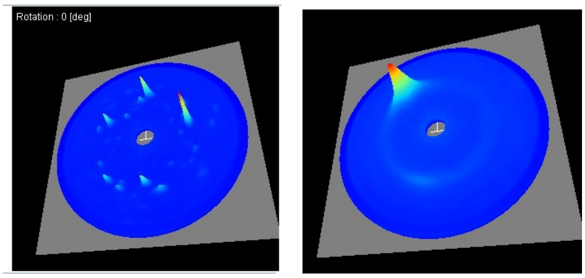

Figure 4: 3D Debye rings data for Stellite sample (coarse grain size) and stainless-steel sample (preferred orientation) [7].

Discussion and Conclusions

Many advances in residual stress measurements obtained using the $Sin^2\psi$ technique have been made over recent decades. These have helped ensure that accurate stress results are obtained on a variety of materials processed under a wide spectrum of conditions. Many aspects of XRD based residual stress measurements have been fully developed and refined including: stress gradients, grain size effects, texture effects, shear stresses, triaxial stresses, two-phase materials, stress in single crystals, and many others. The amount of knowledge acquired over these decades is significant and has helped the scientific community vastly improve the accuracy of their residual stress measurements. All these advances were achieved using the $Sin^2\psi$ technique assuming a triaxial stress tensor.

The SET-Cosα technique however, even today, suffers from the same difficulties the scientific community had experienced decades ago. The SET-Cosα technique theory reported in this paper clearly shows why it is essentially antiquated and relegated to the knowledge level of stress measurements performed in the 1970s, when the effects of shear stress were unknown. Results obtained using the SET-Cosα technique are extremely sensitive to the tilt angle selected when shear stress are present in the material as shown in Figure 2 [7]. Assuming the presence of a biaxial stress state is a huge and unnecessary risk that can lead to erroneous results, especially on materials with large grain size or texture as compared to $Sin^2\psi$ technique [11,12]. The errors associated with SET-Cosα technique can be especially significant when the ratio between the shear stress and the normal stress is high. The solution for Cosα is to use the same assumptions used for the MET-$Sin^2\psi$ technique, i.e., triaxial stress tensor with an adequate number of tilts to cover the full half-space and adequately solve for all of the unknown stress tensor components, and sufficient sampling statistics of d-spacing from the maximum number of grains possible. As this paper has clearly demonstrated, the practitioner cannot assume a priori that the stress field in the material is biaxial before the measurement is performed. Only by assuming a triaxial stress tensor will XRD based residual stress measurements be reliable and accurate using any technique.

References

[1] I. C. Noyan and J.B. Cohen, *Residual Stress, Measurement by Diffraction and Interpretation*, (Springer-Verlag, New York), (1987).

[2] V. Hauk, *Structural and Residual Stress Analysis by Nondestructive Methods*, (Elsevier, Amsterdam), (1997).

[3] ASTM E2860-12, *Standard Test Method for Residual Stress Measurement by X-Ray Diffraction for Bearing Steels*, (2012).

[4] EN 15305, NDT - *Test Method for Residual Stress Analysis by X-ray Diffraction*, (2008).

[5] T. Sasaki, Y. Hirose, K. Sasaki, S. Yasukawa, *Influence of image processing conditions of Debye Scherrer ring images in x-ray stress measurement using an imaging plate*, Adv. X-ray Anal. Vol. 40, (1997), pp.588–594.

[6] N. Peterson, Y. Kobayashi, B.Traeger, P. Sanders, *Assessment and Validation of Cosα Method for Residual Stress Measurement*, Proc. of the ICSP13, (2017), pp. 80-86.

[7] M. Belassel, J. Pineault, M. Bolla, M Brauss, *Evaluation of x-ray diffraction stress instruments using cos-alpha and $sin^2\psi$ techniques in relation to existing standards*, Adv. in X-ray Anal., Vol. 64, (2020), pp.1-10.

[8] M. Belassel, J. Pineault, M. Bolla, M Brauss, *Introducing a triaxial stress field for residual stress measurements using cos-alpha techniques,* Proc. of ICRS11, Nancy, France (2022), (in publication).

[9] J. Ramirez-Rico, S.-Y. Lee, J. J. Ling, and I. C. Noyan, *Stress Measurement Using Area Detectors: A Theoretical and Experimental Comparison of Different Methods in Ferritic Steel Using a Portable X-Ray Apparatus*, J Mater. Sci., Vol. 51, (2016), pp.5343-5355.

[10] K. Tanaka, *The cosα method for X-ray residual stress measurement using two-dimensional detector*, Bulletin of the JSME, Vol. 6, No.1, (2019), pp. 1-15.

[11] C. R. Chighizola, C. R. D'Elia, D. Weber, B. Kirsch, J. C. Aurich, B. S. Linke, M. R. Hill, *Intermethod Comparison and Evaluation of Measured Near Surface Residual Stress in Milled Aluminum*, Exp. Mech., (2021) Vol. 61, pp.1309–1322.
[12] H. Soyama, *Comparison of Various XRD Methods on Evaluation of Residual Stress Introduced by Submerged Laser Peening*, MFN Vol. 19, (2018), pp. 54-56.